Limnol. Oceanogr., 56(4), 2011, 1255–1272

doi:10.4319/lo.2011.56.4.1255

Harmful phytoplankton ecology studies using an autonomous molecular analytical and ocean observing network

J. Ryan,[a,*] D. Greenfield,[b] R. Marin, III,[a] C. Preston,[a] B. Roman,[a] S. Jensen,[a] D. Pargett,[a] J. Birch,[a] C. Mikulski,[c] G. Doucette,[c] and C. Scholin[a]

[a] Monterey Bay Aquarium Research Institute, Moss Landing, California
[b] University of South Carolina, Charleston, South Carolina
[c] National Oceanic and Atmospheric Administration, National Ocean Service, Charleston, South Carolina

Abstract

Using autonomous molecular analytical devices embedded within an ocean observatory, we studied harmful algal bloom (HAB) ecology in the dynamic coastal waters of Monterey Bay, California. During studies in 2007 and 2008, HAB species abundance and toxin concentrations were quantified periodically at two locations by Environmental Sample Processor (ESP) robotic biochemistry systems. Concurrently, environmental variability and processes were characterized by sensors co-located with ESP network nodes, regional ocean moorings, autonomous underwater vehicle surveys, and satellite remote sensing. The two locations differed in their long-term average physical and biological conditions and in their degree of exposure to episodic wind-forced variability. While anomalously weak upwelling and strong stratification during the 2007 study favored toxigenic dinoflagellates (*Alexandrium catenella*), anomalously strong upwelling during the 2008 study favored toxigenic diatoms (*Pseudo-nitzschia* spp.). During both studies, raphidophytes (*Heterosigma akashiwo*) were detected within a similar range of concentrations, and they reached higher abundances at the relatively sheltered, stratified site. During 2008, cellular domoic acid reached higher concentrations and was far more variable at the shallower ESP node, where phytoplankton populations were influenced by resuspended sediments. Episodic variability caused by wind forcing, lateral mixing, internal waves, and subsurface phytoplankton layers influenced ESP detection patterns. The results illustrate the importance of mobilizing HAB detection on autonomous platforms that can intelligently target sample acquisition as a function of environmental conditions and biological patch encounter.

Far-reaching effects of harmful algal blooms (HABs)—on ecosystem and human health and on the viability of fisheries, aquaculture, and tourism—motivate greater understanding of natural and anthropogenic factors modulating HAB dynamics (Ramsdell et al. 2005; Jewett et al. 2008). The Science Plan for the international program Global Ecology and Oceanography of Harmful Algal Blooms (Glibert and Pitcher 2001) identifies the core requirement of "specialized and highly resolving measurements to observe and describe the biological, chemical, and physical interactions that determine the population dynamics of individual species in natural communities." Improving techniques for monitoring and early detection of HABs and gaining a better understanding of how HABs are ultimately linked to larger oceanographic and biological processes are recognized as research priorities (ORION Executive Steering Committee 2005; Jewett et al. 2008). To that end, programs have been initiated that combine data collected from a variety of sources, such as moored and mobile in situ sensors, satellite imagery, shore- and ship-based sample collections, and cabled observatories (Babin et al. 2008; Trainer et al. 2009). As part of that overall effort, field-deployable instruments and handheld kits are being developed and employed to expedite the detection of phytoplankton species and associated toxins, thereby reducing the need for returning samples to a laboratory for analysis (Babin et al. 2005; Casper et al. 2007; Campbell et al. 2010). One instrument that enables autonomous in situ detection of plankton and the harmful substances they may produce is the Environmental Sample Processor (ESP). The ESP uses molecular probe technology to detect a variety of organisms remotely, including marine bacterioplankton, invertebrates, and HAB species (Greenfield et al. 2008; Preston et al. 2009; Scholin et al. 2009), as well as the phycotoxin domoic acid (DA) (Doucette et al. 2009). Previous work with the ESP has focused on method development and instrument validation trials. Here we present results from the first applications of ESP networks to HAB ecology research within an ocean observing system framework.

The study region, Monterey Bay, California (Fig. 1), is a highly dynamic and productive coastal upwelling environment in the central California Current System (CCS). Wind-driven upwelling in the CCS greatly enhances nutrient supply to the euphotic zone and, thus, primary productivity. Sheltered conditions occur in northern Monterey Bay as a result of its recessed position oceanographically—in the lee of the Point Año Nuevo upwelling center (Fig. 1)—and meteorologically, in the lee of the Santa Cruz Mountains; this situation reduces the northern Bay's exposure to strong northwesterly wind forcing (Breaker and Broenkow 1994). These effects of coastal geomorphology are largely responsible for a phenomenon known as the Monterey Bay 'upwelling shadow' (Graham and Largier 1997). Prolonged residence time and weak wind mixing in northern Monterey Bay promote local heating, evident as warm surface temperature (Fig. 1a). Phytoplankton populations thrive

* Corresponding author: ryjo@mbari.org

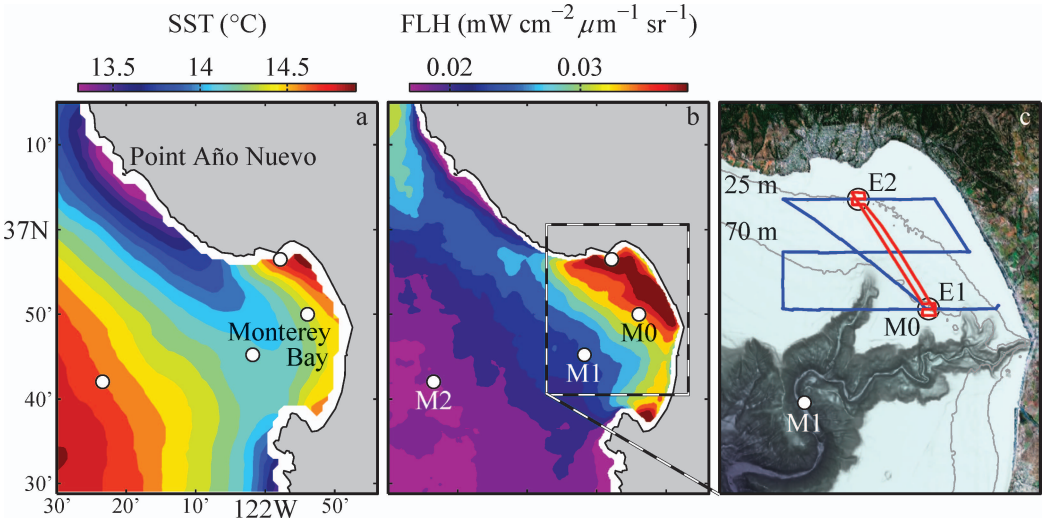

Fig. 1. Environmental setting and ESP network experiment design. Satellite-observed (a) SST and (b) chlorophyll FLH are climatologies of August–November data from 2003–2008. Moorings M0 (70-m water depth), M1 (1200-m water depth), and M2 (1800-m water depth) provided regional meteorological and oceanographic data. (c) Bathymetry in the bay is shown relative to the ESP network node locations E1 and E2 and the AUV survey tracks during the 2007 (blue) and 2008 (red) experiments. The isobaths on which E1 and E2 were placed are contoured and labeled.

on episodic nutrient supply within these sheltered waters (Fig. 1b), and different types of phytoplankton blooms incubate within this area and may rapidly spread from there (Kudela et al. 2008; McManus et al. 2008; Ryan et al. 2008*b*).

Among the HAB species that are often present and may bloom in Monterey Bay are toxigenic diatoms of the genus *Pseudo-nitzschia* (Scholin et al. 2000; McManus et al. 2008); dinoflagellates, including *Cochlodinium fulvescens*, *Alexandrium catenella,* and *Akashiwo sanguinea* (Curtiss et al. 2008; Jessup et al. 2009; Ryan et al. 2010*a*); and the raphidophyte *Heterosigma akashiwo* (O'Halloran et al. 2006; Greenfield et al. 2008). A recent shift in the dominant phycotoxin producers in northern Monterey Bay, from diatoms toward dinoflagellates, has been documented (Jester et al. 2009).

The primary objectives of this study were to detect and estimate the abundance of several HAB species and an algal biotoxin simultaneously in different locations using a network of ESP instruments and to examine HAB species ecology by integrating ESP network observations with environmental data from in situ and remote sensing. Two ESPs were deployed, one at each of two sites expected to experience different oceanographic conditions and phytoplankton communities. These sites were located along the southern and northern peripheries of the Monterey Bay upwelling shadow (Fig. 1). Site E1, along the southern periphery, was more subject to episodic variability of intruding water masses transported into the bay during upwelling- and downwelling-favorable wind forcing (Graham and Largier 1997; Ramp et al. 2005; Ryan et al. 2009). Site E2, along the northern periphery, was nestled within an area expected to be more insulated from regional mesoscale dynamics (Ryan et al. 2008*b*). Additional in situ observations were provided by observing system moorings M0, M1, and M2 (Fig. 1b), an autonomous moored vertical profiler deployed at E2 during the 2007 experiment, and an autonomous underwater vehicle (AUV) that provided synoptic multidisciplinary observations around and between the ESP sites during both experiments (Fig. 1c).

Each ESP was equipped with molecular probe arrays to detect key HAB species that are problematic in coastal regions globally, including toxic diatom species of the genus *Pseudo-nitzschia*, the dinoflagellate *A. catenella*, and the raphidophyte *H. akashiwo* (Greenfield et al. 2006, 2008). Each ESP also carried protein arrays to detect the phycotoxin DA, which is produced by toxigenic *Pseudo-nitzschia* spp. and is a well-established threat to humans and wildlife. The organisms targeted by ESP are often present in Monterey Bay at concentrations below the levels at which HAB events and their effects typically occur, and previous studies have shown that ESP can detect the targeted HAB species at these sub-harmful levels (Greenfield et al. 2008). Presence of multiple HAB species and occasional blooms that can affect marine food webs make Monterey Bay an ideal location for exploring the application of ocean observing systems to autonomously detect HAB species and toxins and to study environmental forcing of HAB events. This study highlights the challenges associated with forecasting the development and distribution of nascent HABs in regions where multiple causative species occur, and it illustrates the prospective utility of using molecular analytical techniques in a remote context to reveal potentially harmful organisms well before associated negative effects may arise.

Methods

ESP network sampling—The procedure by which the ESP collects and processes whole water samples in situ has been described previously (Jones et al. 2008; Preston et al.

2009; Scholin et al. 2009). Preparation of HAB deoxyribonucleic acid (DNA) probe arrays (henceforth 'HAB array') for use with sandwich hybridization assays (SHA; after Scholin et al. 1999) aboard the ESP followed the method of Greenfield et al. (2006), with modifications for normalization of conjugate activity and Optitran BA-S 83 Reinforced Nitrocellulose Membrane (Whatman, Schleicher & Schuell) according to Greenfield et al. (2008). HAB arrays used SHA capture probes for *Pseudo-nitzschia australis* (auD1); *Pseudo-nitzschia multiseries* (muD1); *Pseudo-nitzschia multiseries*; *pseudodelicatissima* (muD2); *H. akashiwo* (Het1); *A. catenella* (NA1); and a control probe (AlexComp) that was diluted 1 : 1000. The sequences for all DNA probes used in this study (capture and signal), as well as standard curves used to calculate approximate cells per liter from completed HAB arrays, can be found in Greenfield et al. (2008).

The limit of detection (LOD) for each capture probe on the HAB array is defined operationally, based upon data from Greenfield et al. (2008), as 3 standard deviations above the array background. This approach has been used previously for SHA in the plate format (Mikulski et al. 2008). For probe auD1 (*P. australis*), the LOD is $\sim$ 380 cells mL^{-1} of homogenate, assuming 2 mL of lysis buffer is used to generate a lysate. This translates to $\sim$ 760 cells for a 1-liter sample taken by the ESP. The LOD for probe muD1 (*P. multiseries*) is $\sim$ 2348 cells mL^{-1} of homogenate or $\sim$ 4696 cells L^{-1} ESP sample. The LOD for probe muD2 (*P. multiseries*; *pseudodelicatissima*) is $\sim$ 1372 cells mL^{-1} homogenate or $\sim$ 2744 cells L^{-1} ESP sample. The LOD for probe Het1 (*H. akashiwo*) is $\sim$ 760 cells mL^{-1} homogenate or $\sim$ 1520 cells L^{-1} ESP sample. The LOD for probe NA1 (*A. catenella*) is $\sim$ 52 cells mL^{-1} homogenate or $\sim$ 104 cells L^{-1} ESP sample.

The methods for extracting DA from *Pseudo-nitzschia* cells and quantification of DA levels using a competitive enzyme-linked immunosorbent assay (cELISA) technique onboard ESP followed the method of Doucette et al. (2009). The cELISA limit of detection (in-water DA concentration; sample volume 1 liter) was $\sim$ 2 ng L^{-1}. As a result of problematic cELISA calibrations for E1 during the 2007 study, toxin quantification was possible only at E2. The 2007 E2 DA results were published in demonstrating the method (Doucette et al. 2009), so here we present DA results only for 2008.

ESP network deployments took place during 30 August–26 September 2007 and 04–24 October 2008. During each study ESPs were deployed at the same two locations and were programmed to collect samples synchronously. The sites for ESP deployment were located relative to average conditions derived from satellite data (Fig. 1; satellite methods described below). Site E1 (36.83°N, 121.90°W; bottom depth $\sim$ 70 m) was located along the climatological outer boundary of the warm, chlorophyll-rich waters of northern Monterey Bay. Site E2 (36.93°N, 121.97°W; bottom depth $\sim$ 25 m) was placed closer to shore, within an area of the warmest, most chlorophyll-rich 'upwelling shadow' waters. HAB arrays were run on whole water (up to 1-liter) samples. Shortly following completion of each HAB array, the ESPs collected and processed samples for DA quantification. The offset between the starts of HAB and DA sample acquisition ranged between 2 h and 3 h. HAB and DA array images and instrument log data were periodically uploaded to a shore station using radio telemetry.

Moored environmental sensors—To unambiguously describe environmental attributes of ESP sampling, measurements exactly co-located with each ESP are essential. Each ESP was deployed with (1) a Sea-Bird Electronics (SBE) 16+ conductivity–temperature–depth (CTD) sensor, (2) a Turner Designs Cyclops-7 chlorophyll fluorometer, (3) a WetLabs C-star transmissometer, and (4) an in situ ultraviolet spectrophotometer (ISUS) for quantification of nitrate (Johnson and Coletti 2002). All sensors were routinely maintained and calibrated. Chlorophyll fluorometers were calibrated by the manufacturer using standards from extracted spinach chlorophyll. Environmental measurements were taken every 20 min and uploaded to a shore station along with ESP array images and instrument log data.

Environmental sensing was augmented by meteorological and oceanographic measurements at long-term mooring sites M0, M1, and M2 (Fig. 1). In this study we used wind observations at M2 and sea surface temperature (SST) measurements at M1 and M0 to examine regional wind forcing and oceanographic responses. Winds were measured with an RM Young 5103 Wind Monitor, and SST was measured with SBE 37 MicroCAT CTD sensors at 1-m depth. Mooring M0 was $\sim$ 500 m west of E1 (Fig. 1c). During the 2007 study, an autonomous moored vertical profiler (MVP; Ryan et al. 2008*a*) was placed $\sim$ 50 m from E2. The profiler acquired hourly high-resolution vertical profiles of physical and optical properties using a Sea-Bird 19 CTD and a WetLabs BB2F backscattering and chlorophyll fluorescence sensor.

AUV surveys—The AUV *Dorado* was repeatedly deployed to survey northern Monterey Bay during each experiment (Fig. 1c). Physical, chemical, and optical sensors on the AUV (Ryan et al. 2009) provided multidisciplinary observations with sufficient resolution and synoptic coverage to describe hydrographic variability and phytoplankton patchiness around and between the ESP nodes. The same chlorophyll fluorometer with the same calibration was deployed on the AUV in both studies presented here. This fluorometer was calibrated in a laboratory facility using standards from extracted spinach chlorophyll. In all surveys the AUV executed sawtooth profiling to map vertical sections along the tracks shown in Fig. 1c. During the 2007 experiment, the AUV survey was designed to provide broad-scale coverage of the entire northern bay. Profile depth tracked bottom depth, and the AUV remained $\sim$ 5 m above bottom at the lower inflection points. During the 2008 experiment the AUV survey was designed to provide higher temporal and spatial resolution. This was achieved with small-scale volume surveys around each ESP and a section between them (Fig. 1c). For each mission, the AUV completed two round-trip surveys. To achieve higher horizontal resolution, we constrained survey depth to 35 m in deeper waters ($>$ 40 m).

Satellite remote sensing—This study used remote sensing data from the Moderate Resolution Imaging Spectro-

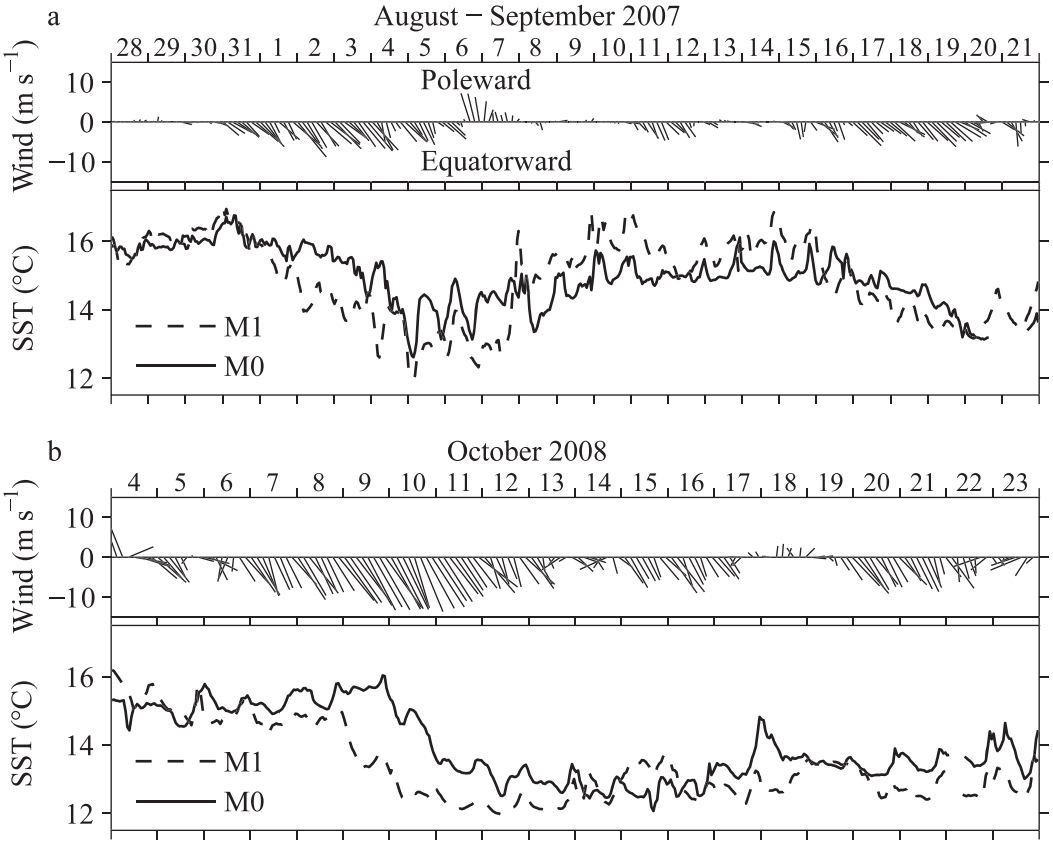

Fig. 2. Regional wind forcing measured at mooring M2 (Fig. 1) and SST from moorings M1 and M0 (Fig. 1) during each ESP network experiment. The vertical scales are the same to facilitate comparison of differences between the (a) 2007 and (b) 2008 study periods.

radiometer (MODIS) Aqua satellite sensor for two purposes: to define average conditions (Fig. 1), which were in turn used to determine where to place ESP nodes, and to examine differences in regional conditions during the two study periods. The processing methods for this MODIS data set are documented (Ryan et al. 2009). Chlorophyll fluorescence line height (FLH) is a proxy for phytoplankton abundance, and previous studies have shown that results from this linear-baseline algorithm better represent patterns of intense phytoplankton blooms in Monterey Bay than do results from band-ratio chlorophyll algorithms (Ryan et al. 2009). To illustrate regional upwelling response during the 2008 study, we use SST images from the Advanced Very High Resolution Radiometer (AVHRR) constellation of sensors, which can provide greater temporal resolution than MODIS SST. The methods of AVHRR processing are documented (Ryan et al. 2010*b*).

Results

Environmental conditions during the 2007 and 2008 ESP network deployments—Upwelling-favorable (equatorward) winds were stronger and more persistent during the 2008 study compared to the 2007 study (Fig. 2). Quantified relative to the 1992–2009 monthly climatology at M2, alongshore equatorward (upwelling-favorable) winds were weaker than average (by 27%) during the 2007 study and stronger than average (by 55%) during the 2008 study. The lag between equatorward wind forcing and appearance of the coolest SST at M1 and M0 is due to the time required for transport of cold waters from their origin in the Point Año Nuevo upwelling center (Fig. 1a; Rosenfeld et al. 1994). The first upwelling pulse during each experiment caused SST decreases at M1 and M0: 31 August to 05 September 2007 and 09–11 October 2008. While the magnitudes of SST decreases were similar during each study, ~ 4°C, cooling occurred more rapidly and was more persistent in 2008 (Fig. 2). Vertical thermal stratification, a key influence on phytoplankton ecology, differed accordingly. The average temperature difference between the surface and 10-m depth at M0 (E1) during the 2008 study was 51% of that in 2007.

The stronger and more persistent upwelling during 2008 (Fig. 2) was pronounced in regional SST, which was cooler throughout the bay, compared with 2007 (Fig. 3a,b). Chlorophyll FLH was also higher throughout the bay during the 2008 study (Fig. 3c,d). The pattern of this difference may be related not only to stimulation of phytoplankton growth by greater influx of upwelled nutrients during the 2008 study but also to intrusion of low-chlorophyll waters into the southern bay during the 2007 study. Similar patterns of low-chlorophyll, low-salinity intrusions result from wind relaxations and reversals (Ryan et al. 2008*a*, 2009, 2010*a*). The 2007 study

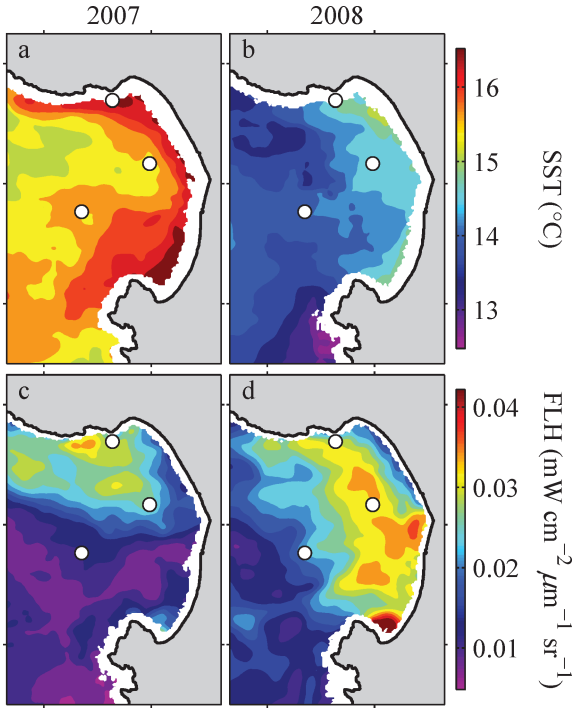

Fig. 3. Satellite-derived SST and chlorophyll FLH averaged for each ESP network deployment. Mooring locations are as in Fig. 1.

was marked by a strong poleward wind event during 06–07 September and by greater persistence of complete wind relaxation (Fig. 2a). Low-chlorophyll waters prevailed at M1 (Fig. 3c), and water column data from M1 clearly showed a strong low-salinity event during 07–17 September (http://dods.mbari.org/lasOASIS/).

The regional variability observed by in situ and remote sensing (Figs. 2, 3) was evident in the conditions measured by the sensors co-located with E1 and E2 (Table 1; Figs. 4, 5). Conditions were colder at the depth of the ESPs during the stronger upwelling of 2008. Coincident lower nitrate and higher chlorophyll concentrations during 2008 indicate more effective nutrient utilization by phytoplankton. During 2007, the particularly high average nitrate at E1 (Table 1) was associated with a gradual increase in nitrate and chlorophyll concentrations during the second half of the experiment (Fig. 4b,c). These high nitrate values at the depth of E1 were confirmed with independent nitrate measurements from an ISUS sensor on the AUV. The gradual nature of the nitrate increase is consistent with the gradual cooling of the second upwelling pulse during the second half of the experiment (Figs. 2a, 4a,b).

Overview of ESP detection of HAB species and toxin—The different oceanographic conditions during the two studies coincided with distinct patterns of HAB species detection by ESP molecular assays. During 2007, signals of HAB species were almost entirely constrained to *A. catenella* and *H. akashiwo* (Fig. 4e,f). A single quantifiable signal for *P. multiseries*; *pseudodelicatissima* occurred at E1 on 18 September (Fig. 4d). This coincided with the second regional upwelling response of the study, which was distinguished from the first in that it was more gradual and persistent, as evident by the temperature, nitrate, and chlorophyll (Figs. 2a, 4a–c).

In contrast, HAB species detection during 2008 was dominated by signals of *Pseudo-nitzschia* spp. at both sites. *P. australis*, *P. multiseries*; *pseudodelicatissima*, and DA concentrations showed similar temporal patterns through a ~ 10-d pulse that followed the arrival of cold, nutrient-rich waters at both sites (Fig. 5a–f). Although *P. australis* were not detected at either site until after the start of the upwelling influence, quantifiable signal for probe muD2 indicated that low concentrations of at least one member of the *P. multiseries*; *pseudodelicatissima* species complex were present at E1 prior to the upwelling pulse. Peak cell concentrations were an order of magnitude higher for *P. multiseries*; *pseudodelicatissima* than for *P. australis* during 2008 (Fig. 5e,f) and nearly an order of magnitude greater than the single detection of the 2007 deployment (Figs. 4d, 5f). A pulse in *H. akashiwo* abundance was observed at E2 following the pulse in *Pseudo-nitzschia* spp. populations (Fig. 5e–g). The ranges of cell concentrations for *H. akashiwo* in the two studies were comparable (Figs. 4f, 5g). Unlike in 2007, *A. catenella* were not detected during 2008.

Integration of 2007 molecular and environmental observations—Bay-wide conditions mapped by AUV during the 2007 study showed strong variation in stratification, the presence and intermixing of regional water types, and phytoplankton abundance (Fig. 6). During the earlier part of the study, thermal stratification was relatively weak around E1 and relatively strong around E2 (Fig. 6a, 04–05 September). A low-salinity lens was evident around E1 early in the experiment, and intrusion of low-salinity waters into the study site was much stronger toward the end of the experiment (Fig. 6b). E1 was more affected by low-salinity intrusions during the early and late phases of the study. Chlorophyll concentrations were higher throughout the study region toward the end of the experiment, particularly around E1 (Fig. 6c).

Table 1. Average conditions at ESP network nodes E1 and E2 (Fig. 1) during each deployment. The time-series data are presented in Figs. 4 and 5.

	Depth (m)		Temperature (°C)		Salinity		Nitrate (μmol L^{-1})		Chlorophyll (μg L^{-1})	
Year	E1	E2	E1	E2	E1	E2	E1	E2	E1	E2
2007	10.7	10.6	13.7	13.3	33.5	33.6	12.2	6.7	3.9	3.8
2008	10.8	4.6*	12.7	13.3	33.5	33.5	5.3	5.5	7.8	6.7

* Shallow depth of E2 during 2008 affected average properties.

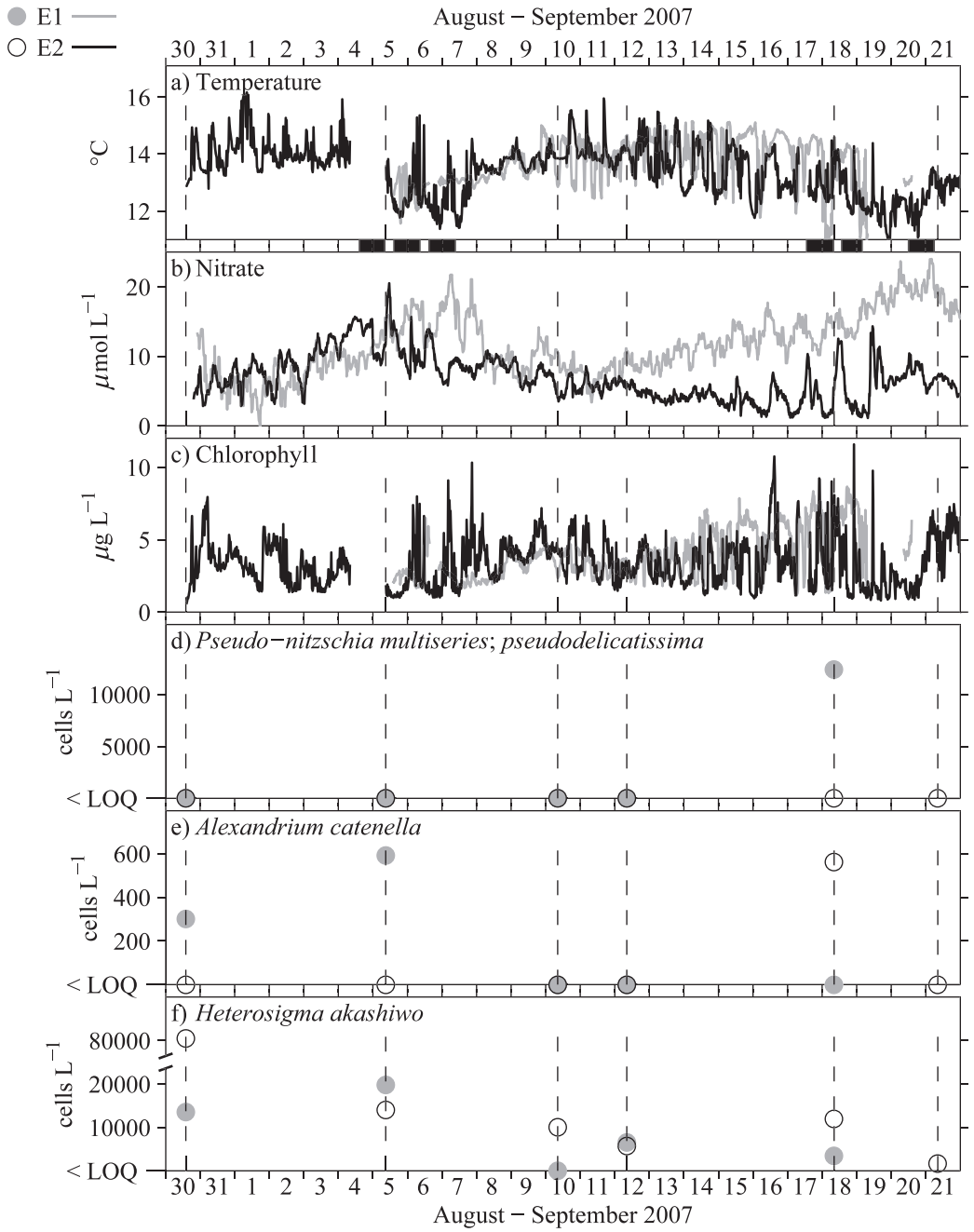

Fig. 4. (a–c) ESP environmental data (20-min resolution) and (d–f) HAB detection results at both ESP network nodes during the 2007 experiment. E1 operations ended one sample before E2. The label <LOQ indicates below the level of quantification for the ESP molecular probes. The filled periods (horizontal bars) between the temperature and nitrate plots indicate the times of AUV surveys (Figs. 6, 7, 9, 12).

The maximum signals of both *A. catenella* and *H. akashiwo* at E1 co-occurred on 05 September (Fig. 4e,f). AUV sections on 04 and 05 September show that E1 resided in the thermocline and sampled near the base of a low-salinity lens, where a subsurface chlorophyll maximum persisted (Fig. 7). The chlorophyll fluorescence maximum around E1 coincided with a maximum in particle backscattering (not shown), indicating that it was a true phytoplankton biomass maximum and was not caused by quenching of fluorescence near the surface (Cullen and Eppley 1981; Holm-Hansen et al. 2000).

The only quantifiable *Pseudo-nitzschia* spp. signal during the 2007 study occurred on 18 September at E1 (Fig. 4d), when chlorophyll concentrations were elevated (Figs. 4c, 6c). Environmental sensor data show that this sample was acquired immediately following a period of rapid temperature change (2.7°C increase in 20 min), coincident with similarly rapid increases in chlorophyll and salinity (Fig. 8).

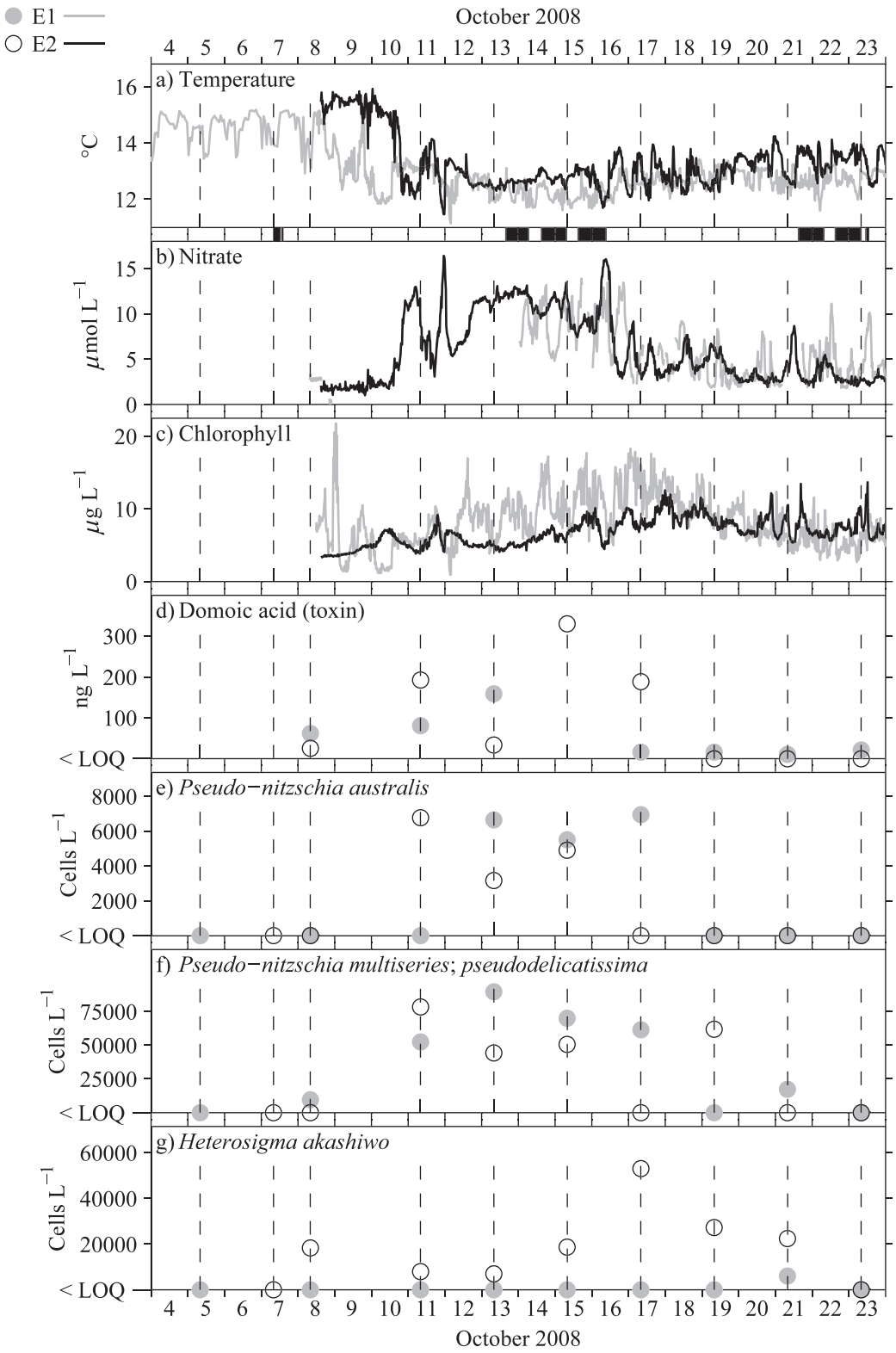

Fig. 5. (a–c) ESP environmental data (20-min resolution) and (d–g) HAB detection results at both ESP network nodes during the 2008 experiment. All environmental data are from sensors co-located with ESP, except E1 temperature during 04–07 October, which is from mooring M0 at 10-m depth (500 m west of E1). The label <LOQ indicates below the level of quantification for the ESP molecular probes. The filled periods (horizontal bars) between the temperature and nitrate plots indicate the times of AUV surveys (Fig. 15).

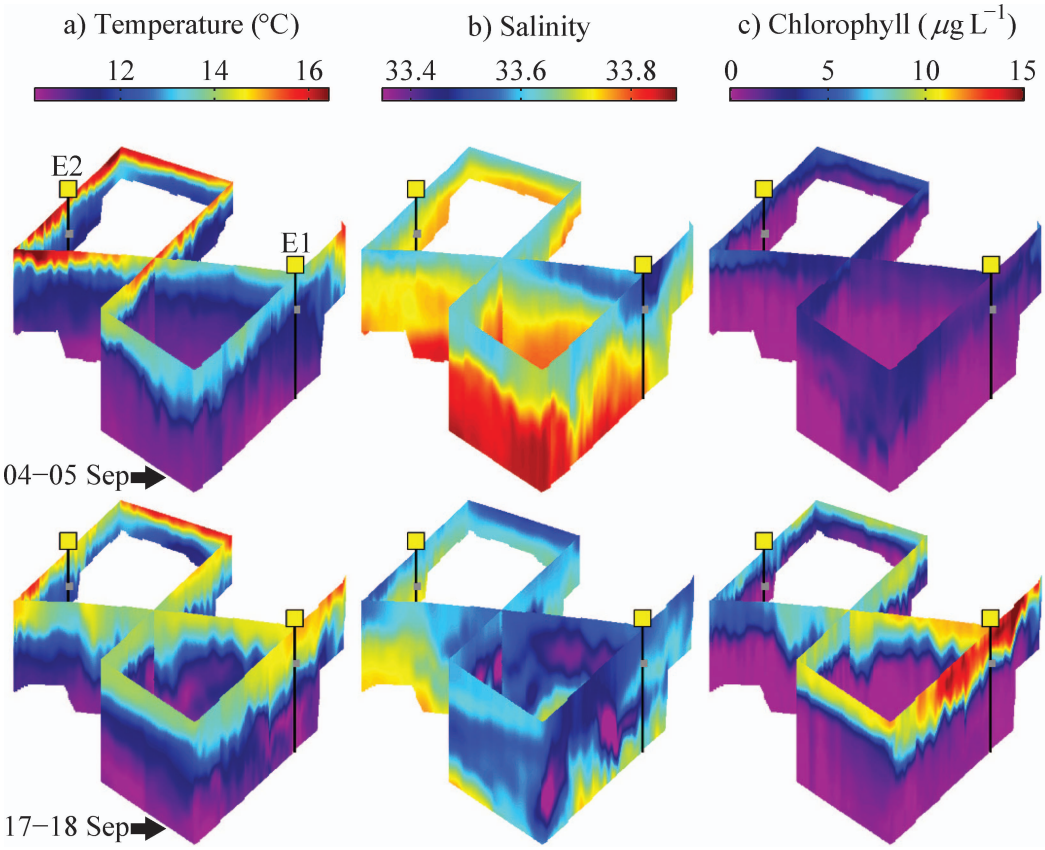

Fig. 6. (a,b) Hydrographic and (c) bio-optical conditions near the start (top row) and end (bottom row) of the 2007 ESP network experiment. ESPs are represented as gray boxes on the mooring lines. The AUV survey track is shown in Fig. 1c, and the depth range shown is 2–35 m. Each survey comprised more than 750 profiles acquired in ~ 18 h. Each survey was started in the southeastern corner, east of E1, in the early afternoon and was completed approximately 2 h after sunrise the next day at E1. Because both surveys followed the same spatial pattern on the same daily schedule, comparison of fluorometric chlorophyll levels at the same places along each survey is not confused by effects of diel light variation on the quantum yield of fluorescence.

AUV sections on 17–18 September show that E1 resided in the strong thermal and biological gradients of the thermocline (Fig. 9). A low-salinity lens evidently advected onshore between 17 and 18 September, such that the lens and a corresponding cold anomaly resided directly below E1 (Fig. 9b). Thus, the rapid environmental changes preceding the *P. multiseries*; *pseudodelicatissima* detection at E1 (Fig. 8) were likely caused by movement of the cold, low-salinity lens relative to E1 (Fig. 9). Sample acquisition was evidently from the base of the warmer, more saline, and chlorophyll-rich mixed layer.

The only quantifiable signal of *A. catenella* at E2 occurred on 18 September (Fig. 4e). A series of four sharp peaks in temperature and chlorophyll occurred at E2 beginning early on 18 September, and the ESP sampling that resulted in *A. catenella* detection coincided with the fourth peak (Fig. 10). The sampled peak was associated with a high-frequency shift in water column structure, consistent with the passage of an internal wave (Fig. 11). A near-concurrent synoptic AUV map shows internal waves across a range of scales around E2 on 18 September (Fig. 12). We interpret that depression of the shallow waters by an internal wave (Fig. 12) caused the thermal and chlorophyll peak during which E2 sampled *A. catenella* (Fig. 11).

The MVP time series adjacent to E2 illustrates the range of frequency across which environmental forcing was occurring at this site (Fig. 13). The two pulses of cold water following the upwelling winds (Fig. 2a) affected temperature, salinity, and chlorophyll of the entire water column at E2 (Fig. 13). Diurnal and semidiurnal variations in water column structure were pronounced throughout the time series. Variation in this frequency band is related to tidal and wind-forced advection (Petruncio et al. 1998; Woodson et al. 2007, 2009). The highest frequency of variability resolved with hourly profiles was due to internal waves (Figs. 10–13). Because E2 resided mostly below the high-chlorophyll, near-surface waters during this deployment (Fig. 13), local vertical movement of plankton populations by internal wave forcing may have been a primary factor in determining ESP sample results.

Integration of 2008 molecular and environmental observations—Exceptionally clear atmospheric conditions during the 2008 study allowed application of satellite remote sensing

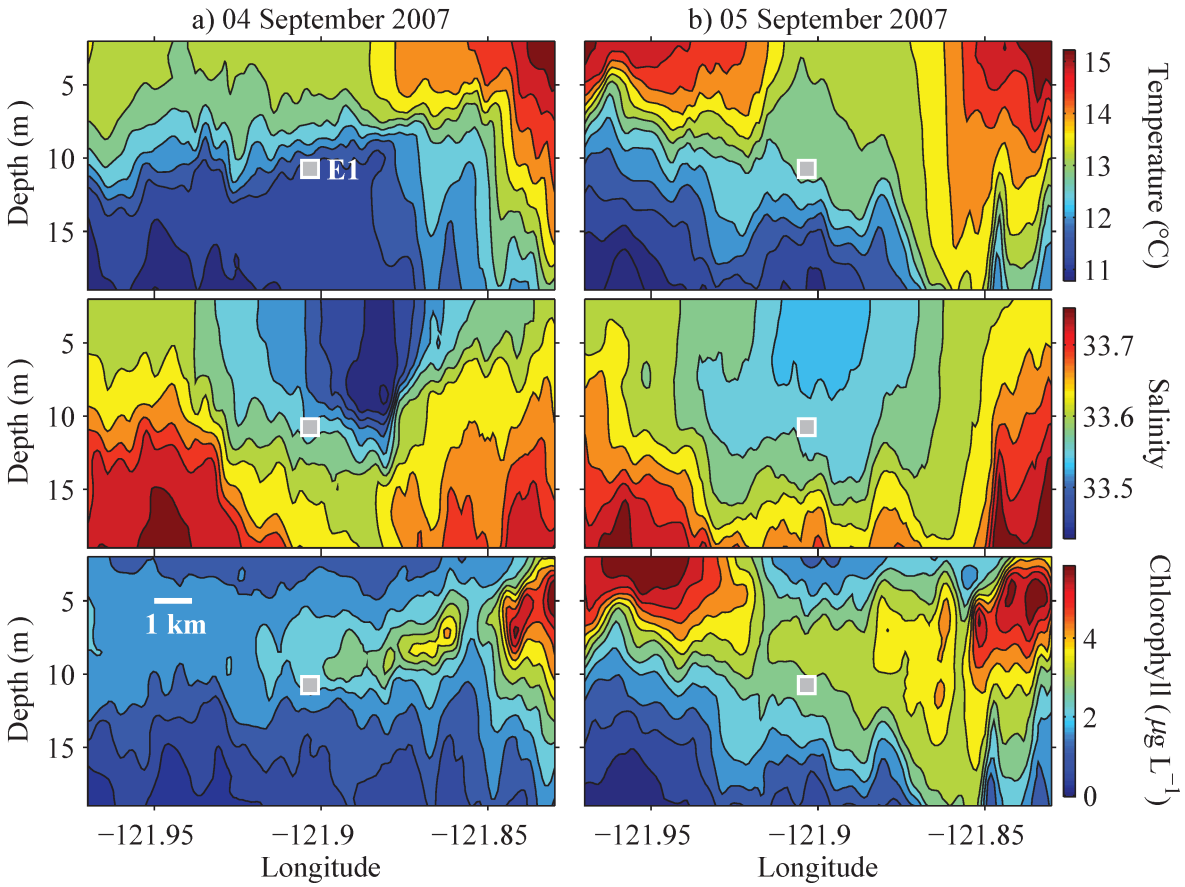

Fig. 7. Synoptic maps of conditions relevant to the E1 detection of *Alexandrium* and *Heterosigma* on 05 September 2007 at E1 (Fig. 4). (a) 04 September AUV survey data were acquired starting ~ 18 h before ESP sample acquisition; (b) 05 September AUV survey data were acquired starting ~ 6 h after ESP sample acquisition. Interpolated vertical sections were derived from 90 profiles acquired in 2.6 h of mid-afternoon, and both surveys followed the same spatial pattern on the same daily schedule. With these sampling attributes, neither description of the spatial patterns in fluorometric chlorophyll concentrations within each section nor comparison between the two sections would be confused by effects of diel light variation on the quantum yield of fluorescence.

to describe development of the strong upwelling pulse (Fig. 2b) throughout the Monterey Bay region (Fig. 14). Although upwelling centers north and south of Monterey Bay were active, the Año Nuevo upwelling center north of Monterey Bay (Fig. 1) supplied upwelled waters to the northern bay ESP network nodes. As indicated by remote sensing (Fig. 14) and in situ observations (Fig. 5), E1 and E2 were similarly affected by the advected upwelled waters. Consistent with the measurements at the ESPs (Fig. 5; Table 1), chlorophyll concentrations mapped by AUV surveys were higher around E1 than E2 (Fig. 15). Elevated chlorophyll concentrations also extended over a greater depth

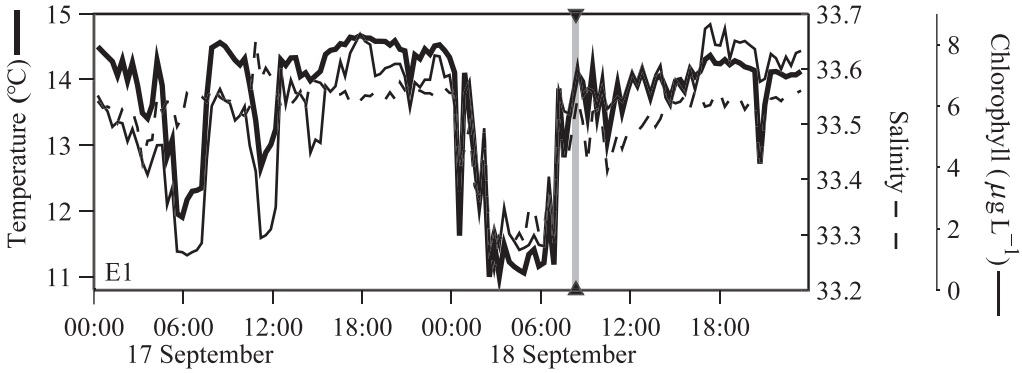

Fig. 8. Temperature, salinity, and chlorophyll concentration at E1 before, during, and following the 18 September 2007 detection of *Pseudo-nitzschia multiseries*; *pseudodelicatissima* (Fig. 4d). The vertical gray bar shows the E1 sample intake period.

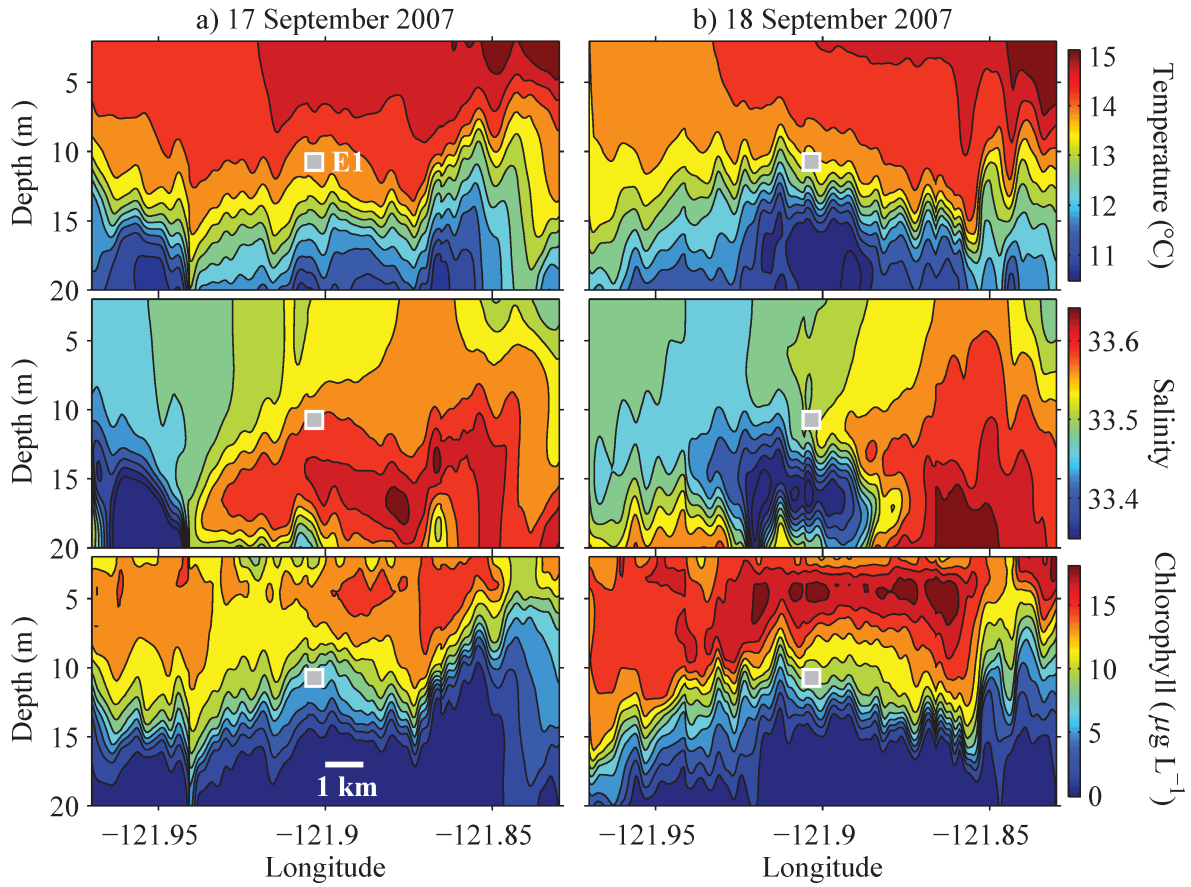

Fig. 9. Synoptic maps of conditions relevant to the detection of *Pseudo-nitzschia multiseries*; *pseudodelicatissima* at E1 on 18 September 2007 (Fig. 4d). (a) 17 September AUV survey data were acquired starting ~ 19 h before ESP sample acquisition; (b) 18 September AUV survey data were acquired starting ~ 5 h after ESP sample acquisition. Interpolated vertical sections were derived from 92 profiles acquired in 2.7 h of mid-afternoon, and both surveys followed the same spatial pattern on the same daily schedule. With these sampling attributes, neither description of the spatial patterns in fluorometric chlorophyll concentrations within each section nor comparison between the two sections would be confused by effects of diel light variation on the quantum yield of fluorescence.

range at E1, which was located adjacent to the strongest frontal gradients caused by the upwelling pulse (Fig. 15a–c).

Despite differences in chlorophyll concentrations and vertical distributions at E1 and E2 (Figs. 5c, 15), *Pseudo-nitzschia* spp. abundance estimates from ESP sampling were within a similar range (Fig. 5e,f). At E2 DA concentrations reached higher levels and exhibited greater variability (Fig. 5d; variance higher by a factor of > 5 at E2). Stronger influence of resuspended sediments was also observed at E2, evident in the AUV sections as the columns of highest optical backscattering in the relatively low-chlorophyll waters around E2 (Fig. 15). The coincident

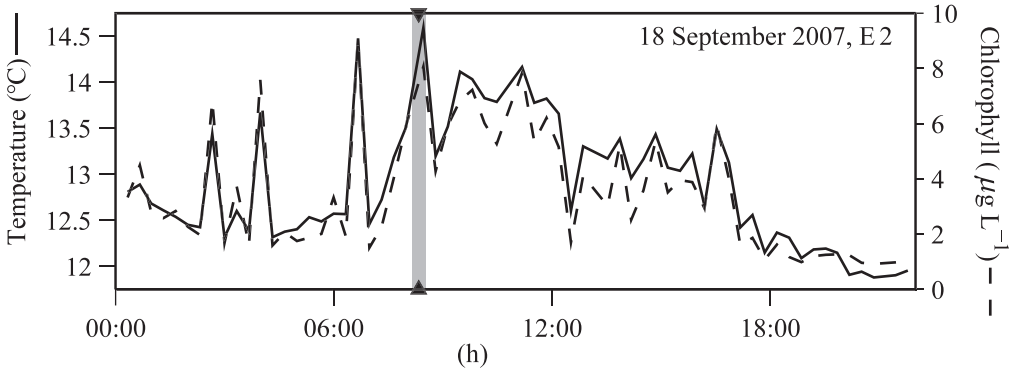

Fig. 10. Temperature and chlorophyll concentration at E2 before, during, and following the 18 September 2007 detection of *Alexandrium* (Fig. 4e). The vertical gray bar shows the E2 sample intake period.

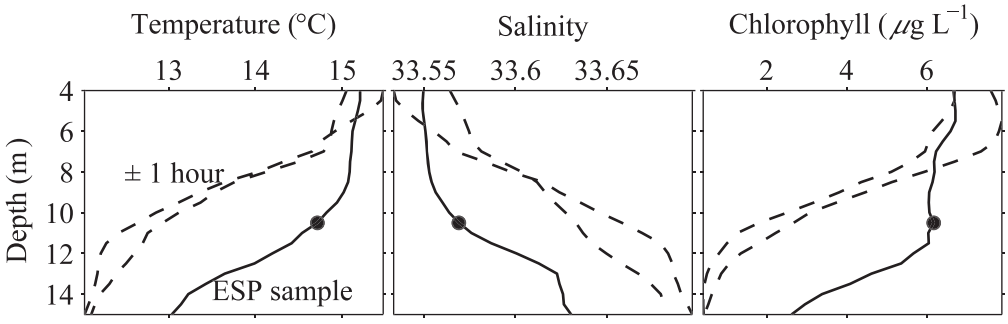

Fig. 11. Water column profiles adjacent to E2, concurrent with the 18 September 2007 sampling of *Alexandrium* (Fig. 10) and ± 1 h.

attributes of high particle backscattering and low chlorophyll fluorescence indicate the prevalence of particles that are not active phytoplankton—likely resuspended sediments.

By 21 October, *Pseudo-nitzschia* spp. and DA signals from the ESP network were either very low or absent (Fig. 5d–f). AUV surveys during 21–22 October showed that major changes in the environment had occurred relative to 13–15 October (compare Fig. 15d,e with Fig. 15a–c). Depletion of nitrate was evident in shallow waters across the ESP network by 21 October (Fig. 15d), consistent with the relatively warm SST (Fig. 14j). Horizontal density and nitrate gradients were significantly diminished, and high-chlorophyll concentrations were limited to relatively small patches (Fig. 15d,e). These high-resolution maps of the changed physical, chemical, and biological fields are consistent with the point measurements at the ESPs (Fig. 5). Resuspended sediments were still evident around E2 (Fig. 15d,e), but their optical signal was weaker than it had been during the primary upwelling response (Fig. 15a–c).

The other HAB array signal during the 2008 study was from *H. akashiwo*, which was present at E2 prior to the upwelling pulse and exhibited increased abundances during and following the pulse in *Psuedo-nitzschia* spp. (Fig. 5g). *H. akashiwo* concentrations were markedly higher at E2 than at E1, and peak concentrations at E2 on 17 October followed a major decline in nitrate concentrations the previous day (Fig. 5b,g). The nitrate and temperature oscillations that occurred on 16–18 October indicate that the mooring was in a frontal zone, and the temperature peak and nitrate trough that coincided with the 17 October sample indicate that the sample was acquired from the warmer, more nutrient-depleted side of the front. Satellite

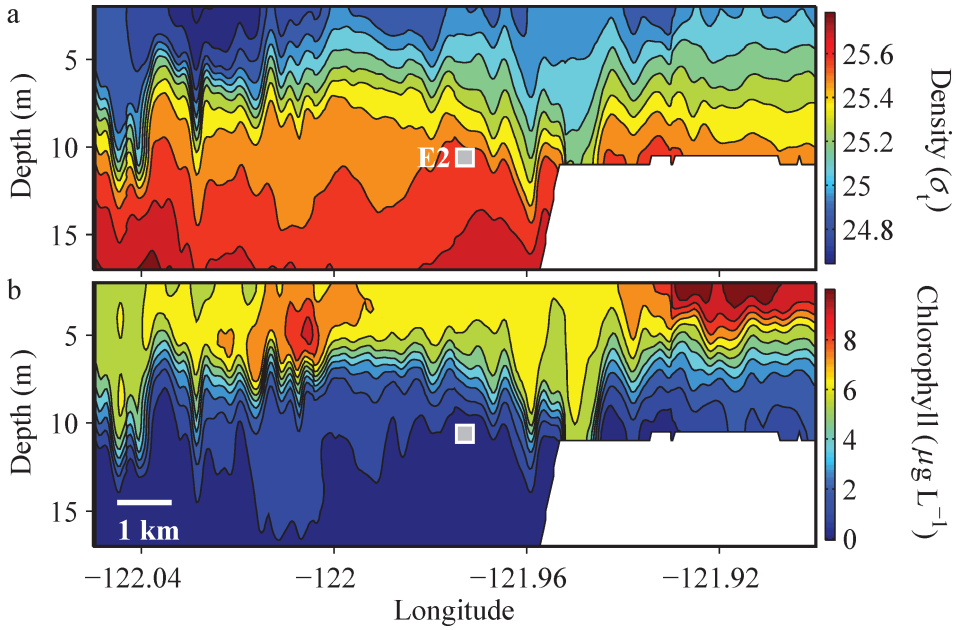

Fig. 12. Synoptic maps of conditions relevant to the detection of *Alexandrium* at E2 on 18 September 2007 (Fig. 4). AUV survey data were acquired starting ~ 6 h before ESP sample acquisition. Interpolated vertical sections were derived from 40 profiles acquired in 1.9 h during dark early morning of 18 September; thus, spatial patterns in fluorometric chlorophyll would not have been strongly influenced by diel variation in the quantum yield of fluorescence.

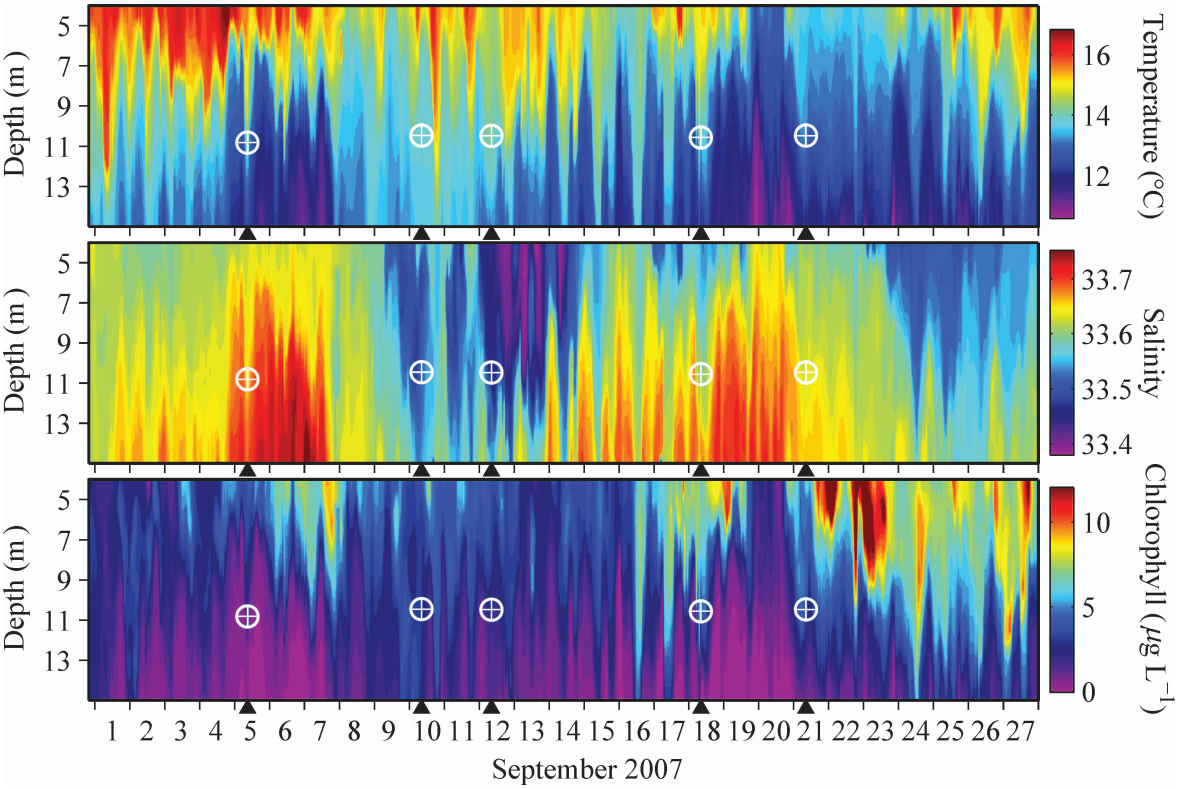

Fig. 13. Hourly water-column profiles at E2 from the autonomous moored vertical profiler.

data from 16 October confirm that E2 was in a frontal zone with warmer, higher chlorophyll waters east of the mooring (Fig. 14i; chlorophyll not shown).

Discussion

The molecular analytical and environmental observing network revealed clear relationships between environmental conditions and HAB species composition in Monterey Bay. A primary environmental factor was the strength of upwelling and associated patterns in stratification. Upwelling was anomalously weak during 2007 and anomalously strong during 2008. At the E1 site, where vertical thermal stratification could be consistently quantified during each study, stratification was likewise greater during 2007 by a factor of 2. *A. catenella*, a motile dinoflagellate presumably favored by relatively strong stratification (Joint et al. 1997; Lechuga-Deveze and Morquecho-Escamilla 1998; Blasco et al. 2003), was only detected during the 2007 study. The motile raphidophyte *H. akashiwo* was detected at much higher abundances at E2 than at E1 during both studies. The E2 node was in the more sheltered area of the Monterey Bay upwelling shadow, which is known to incubate blooms of species favored by stratification (Ryan et al. 2008*b*). In contrast, the strong upwelling pulse at the start of the 2008 study was associated with a distinct pulse in the primary toxigenic diatom genus of the CCS, *Pseudo-nitzschia*. A previous study of multiple sites in the CCS showed the greatest abundance of toxic *Pseudo-nitzschia* spp. and the highest DA levels in waters associated with upwelling zones near coastal headlands (Trainer et al. 2000). Monterey Bay is downstream of an upwelling center at the Point Año Nuevo headland, and this upwelling center was the dominant influence on water mass variability during this study.

Average upwelling intensity in the CCS (Bakun 1973), including more specifically Monterey Bay (Pennington and Chavez 2000), decreases from summer to fall. If upwelling conditions and HAB species composition during our studies were determined primarily by average seasonal variation, we would expect that September 2007 would have experienced stronger upwelling and possibly a stronger signal from HAB diatoms favored by strong upwelling. Instead, we observed the opposite—anomalously strong upwelling and higher HAB diatom signals during the October 2008 study. Because interannual and episodic variations in this region are so great, the observed departure from the expected average seasonal pattern is not surprising. In October 2008, during the second study, the Pacific Decadal Oscillation (PDO) reached its lowest (most negative) level since November 2005. Negative PDO indices are associated with positive upwelling wind stress anomalies and cold SST anomalies along the eastern North Pacific. Although we may speculate that large-scale low-frequency variability may have influenced our results, the substantial analysis required to investigate this possibility is beyond the scope of this article.

While SST at both sites was similarly affected by upwelling events during both studies, there were significant differences between the sites with regard to HAB species composition, utilization of nitrate, and toxin variability. These differences imply the importance of small-scale

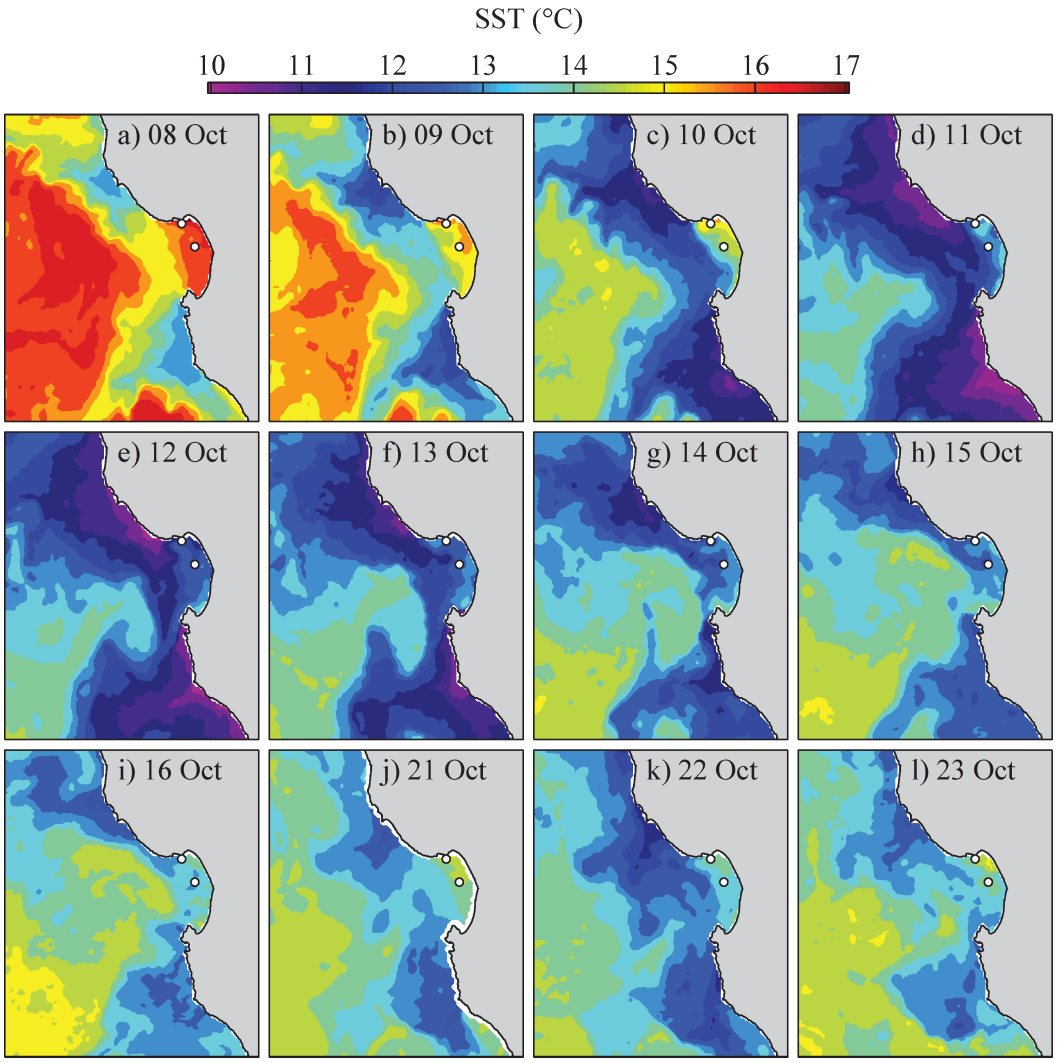

Fig. 14. Development of the coastal upwelling response during the 2008 study, as evident in regional SST.

variability. The environmental observations showed that the patterns of HAB detection by the ESPs were influenced by a variety of episodic processes and small-scale variability. During the 2007 study, maximum signals of both *A. catenella* and *H. akashiwo* at E1 occurred when the ESP sampled a subsurface chlorophyll maximum layer in a frontal zone. Previous studies in Monterey Bay have shown that intense phytoplankton thin layers can form in the upwelling shadow (McManus et al. 2008; Ryan et al. 2010*a*; Sullivan et al. 2010) and that frontal dynamics in this region of the bay, including local nutrient flux and vertical shear, may enhance development of layers (Ryan et al. 2008*a*, 2010*a*). Detection of *A. catenella* at E2 coincided with sampling of an internal wave perturbation at that site, during which the relatively warm, chlorophyll-rich waters of the mixed layer were depressed around the ESP. This may have influenced not only the water around the mooring but also the concentration of phytoplankton in the depressed mixed layer. Previous studies in this region of the bay using in situ and remote sensing have described apparent concentrations of phytoplankton in troughs of internal waves (Ryan et al. 2005*a*,*b*). During the 2008 study, the closer proximity of E1 to the strongest nutrient and density perturbations of an upwelling filament was associated with higher chlorophyll concentrations and a thicker chlorophyll-enriched layer. Also, persistent benthic–pelagic coupling at E2 was associated with greater (5×) variability in cellular DA in *Pseudo-nitzschia* spp. We speculate that the much greater variability in cellular DA was related to the influence of resuspended sediments throughout the water column at E2. Sediments can contain trace metals that influence production of DA by *Pseudo-nitzschia* cells (Rue and Bruland 2001; Maldonado et al. 2002; Rhodes et al. 2006). Moreover, elevated toxin levels are largely supported by adequate nitrate levels, which are required for the synthesis of nitrogen-rich DA (Pan et al. 1998).

Although the complete measurements required to definitively interpret the complex ecological relationships of all detected HAB species were not acquired during our studies (e.g., iron and copper measurements in the resuspended sediments around E2 and their relationship

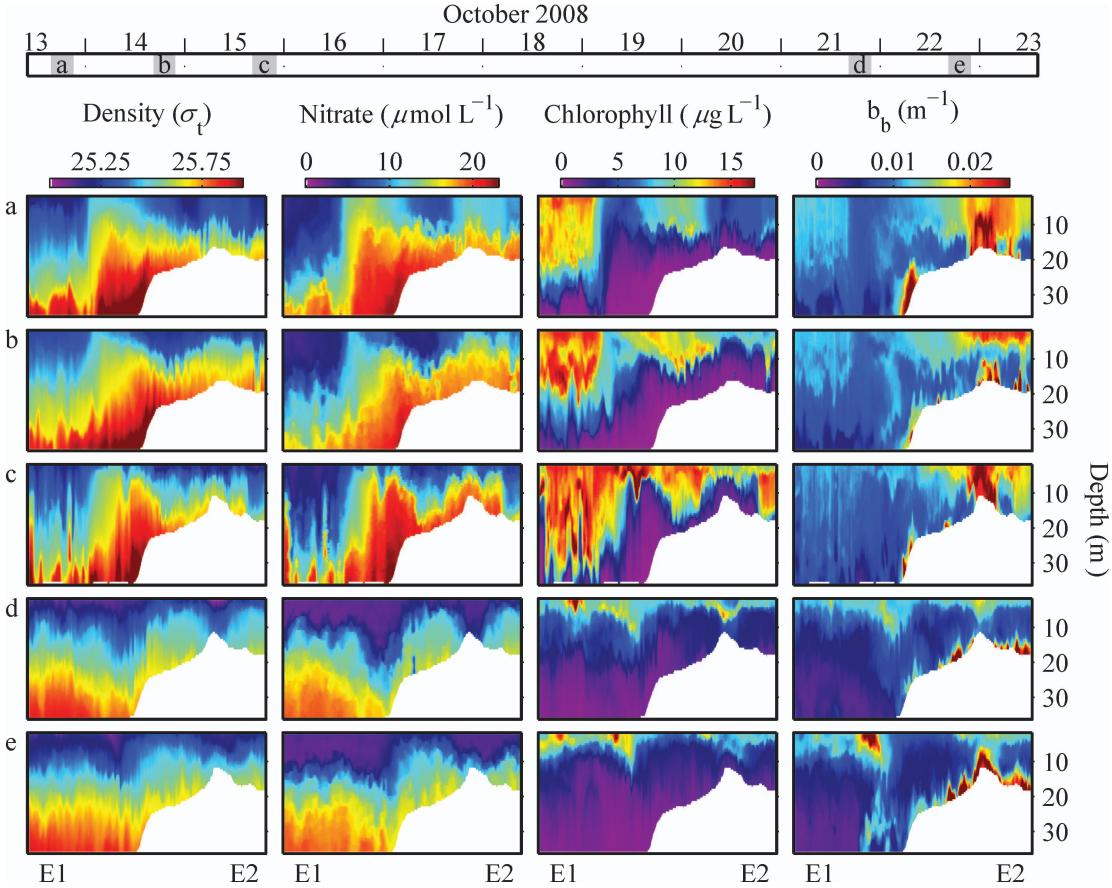

Fig. 15. Synoptic AUV water column maps during the (a–c) peak response to upwelling and the (d, e) subsequent warming. The parameter b_b is optical backscattering at 470 nm. Each interpolated vertical section was derived from ~ 240 profiles acquired in 5 h. Because all surveys followed the same spatial pattern on the same daily schedule, 16:00 h to 21:00 h, comparison of fluorometric chlorophyll levels at the same places along each survey is not confused by effects of diel light variation on the quantum yield of fluorescence. *See* Fig. 5 for continuous records at E1 and E2.

to cellular DA concentrations), the high-resolution environmental data were essential to observe processes that are known to be important to HAB ecology. Further, the glimpses of small-scale influences on HAB population dynamics enabled by these intensive environmental observations motivate advancement of capabilities for adaptive sampling. For HAB species known to aggregate in subsurface layers, targeted mapping and sampling of phytoplankton layers would provide valuable adaptive sampling. This capability has recently been developed and tested using the *Dorado* AUV (Zhang et al. 2010). Similarly, a detection algorithm for intermediate nepheloid layers has been developed and applied to zooplankton ecology studies in Monterey Bay (Ryan et al. 2010*c*).

Fronts represent another key environmental target for adaptive sampling. Phytoplankton ecology is influenced by fronts in a variety of ways, including enrichment of growth conditions (Pingree et al. 1975; Ryan et al. 1999; Smayda 2002), aggregation and transport of biomass (Tester and Steidinger 1997; Ryan et al. 2005*b*; Janowitz and Kamykowski 2006), formation of thin biological layers by vertical shear (Franks 1995; Ryan et al. 2008*a*), and coupling of the mixed layer with the bottom boundary layer (Ryan et al. 2005*a*). Aggregation of biogenic surfactants at fronts has also been linked to a recently discovered mechanism by which dinoflagellate blooms can harm marine life (Jessup et al. 2009). At site E1, the site chosen to represent variability due to influx of different water types, frontal dynamics were pronounced during both studies. During the 2007 study, the maximum signals of both *A. catenella* and *H. akashiwo* coincided with the presence of a complex front in which a phytoplankton layer resided beneath a surface low-salinity lens. This front was associated with a surface slick (indicative of convergence), lateral mixing, and cross-frontal interleaving of water types (Ryan et al. 2010*b*). With the goal of better mapping and sampling fronts, algorithms for autonomous tracking of fronts have been developed and successfully tested in Monterey Bay using the *Dorado* AUV (K. Rajan unpubl.).

In addition to expanding capabilities, observing system design must consider cost efficiency. Different requirements for monitoring and research applications will require different configurations of observing assets. Monitoring at geographically fixed locations is effective when there is prior knowledge of the locations in which potentially harmful organisms incubate, are transported by coastal currents, or will contact human populations or sensitive aquaculture and fisheries resources. This knowledge can be

used to design an efficiently scaled and effective observing program. Autonomous monitoring of water quality affected by pathogens and/or HABs at public beaches may cost effectively use piers as platforms, as has been tested with ESP at the Santa Cruz Municipal Wharf in Monterey Bay. If ocean moorings are required, selection of the number and location of observing nodes can be informed by knowledge of regional HAB ecology. Perhaps the clearest model system illustrating such an approach is that of *Alexandrium* spp. blooms in the Gulf of Maine, where biological and physical controls of bloom inception and regional expansion are well understood (Anderson et al. 2005). Susceptible coastline across three New England states can be effectively monitored by relatively few strategically placed monitoring sites. Because of this efficiency, the first molecular long-term HAB monitoring network is being established in the Gulf of Maine. In regions where HAB ecology is more complex or not as well understood, prioritization and selection of sites for molecular monitoring may be based upon analyses of regional oceanographic and bloom conditions (Ryan et al. 2008*b*; Zhang and Bellingham 2008) and consideration of the most HAB-sensitive sites. Efficiency of molecular observations may be augmented not only by informed spatial planning but also by informed temporal expenditure of in situ molecular sensing resources. While some applications may require fixed-time sampling, such as monitoring of pathogens to inform beach closure on a daily basis, other applications allow more efficient, targeted use of molecular sensing. For example, real-time monitoring of ocean salinity, currents, and chlorophyll concentrations using in situ or remote sensing as well as model predictions (Li et al. 2009) can identify the times during which expenditure of in situ molecular analysis will provide critical information on *Alexandrium* in coastal waters of the Gulf of Maine. While regional observations and model predictions may define alerts, sensors co-located with the molecular detection nodes would provide the most robust basis for the triggering of adaptive sampling and expenditure of molecular resources.

While monitoring at geographically fixed locations will serve monitoring and research needs for HABs in many regions, some HAB research requires targeted patch sampling from mobile platforms. One of the primary conclusions from the research summarized here is that patchy, dynamic coastal waters present an extremely difficult sampling problem for which fixed-point moorings alone may be inadequate. In such complex coastal environments, greater effectiveness and cost efficiency may require focus on mobile AUVs rather than moorings. For example, blooms of toxigenic *Pseudo-nitzschia* incubate offshore in the Juan de Fuca eddy, and these blooms become a coastal management concern when they are transported into Washington coastal waters during storm events (Trainer et al. 2003, 2009). In the case of an offshore source that may approach from a range of directions, an AUV with onboard molecular sensing capabilities could monitor blooms in the periphery of ecologically sensitive sites and provide early warning if toxic blooms approach. AUVs with relatively long endurance would be most appropriate to maintain monitoring presence, and intelligent expenditure of onboard molecular sensing resources would be essential. The next generation of ESP instruments will be significantly smaller than the current generation, allowing for integration with long-range AUVs. Algorithms for targeting sample acquisition with AUVs have been developed for phytoplankton patch sampling (Zhang et al. 2010).

The ecological and socioeconomic effects of HABs motivate development of methods to advance not only the understanding of their ecology but also the ability to effectively and efficiently monitor and predict their occurrence. The molecular analytical and environmental sensing network employed in this study is an example of the integrated observing capabilities needed for this purpose. Simultaneous monitoring of HAB species and toxins enables detection of conditions that are of primary concern to human health—potential vectoring of toxins. This includes ASP toxin–producing *Pseudo-nitzschia* species, which pose health threats at relatively high cell concentrations, as well as PSP toxin–producing *Alexandrium* species, which may cause harm at very low cell concentrations. As for *Pseudo-nitzschia*, tests for *Alexandrium* and their toxins will be deployed together on ESP in the future. Complementing targeted molecular sensing, multidisciplinary, multi-scale observations of environmental variability support a greater understanding of HAB ecology, development of predictive models, and application of predictive models to target applications of observing systems.

Acknowledgments

We thank the engineering technicians and machinists at the Monterey Bay Aquarium Research Institute (MBARI) for their invaluable help and dedication toward instrument development and the MBARI Marine Operations for support of mooring deployments and autonomous underwater vehicle operations. Moderate Resolution Imaging Spectroradiometer (MODIS) data were provided by the National Aeronautics and Space Administration (NASA) Level 1 and Atmosphere Archive and Distribution System. MODIS data processing utilized the SeaWiFS Data Analysis System software and algorithms developed by the MODIS Ocean Biology Processing Group. The Advanced Very High Resolution Radiometer (AVHRR) data shown in Fig. 14 were provided by R. Kudela, UCSC; AVHRR processing was supported by the National Oceanic and Atmospheric Administration (NOAA) CoastWatch and the Central and Northern California Ocean Observing System programs. We thank J. Cullen and an anonymous reviewer for their constructive reviews of the original manuscript. This research was supported by the David and Lucile Packard Foundation. Development and application of the ESP have been funded in part by grants from the David and Lucile Packard Foundation, through funds allocated by MBARI, the National Science Foundation (Ocean Sciences 0314222 and Emerging Frontiers 0424599 to C.S., and Ocean Sciences 0314089 to G.J.D.), NASA (NNG06GB34G to C.S.), and the Gordon and Betty Moore Foundation (ERG731 to C.S.). Funding for mooring M0 support was through the NOAA Center for Integrated Marine Technology (NA160C2936). This manuscript does not constitute an endorsement of any commercial product or intend to offer an opinion beyond scientific or other results obtained by the NOAA. No reference shall be made to NOAA, or this publication furnished by NOAA, to any advertising or sales promotion, which would indicate or imply that NOAA recommends or

endorses any proprietary product mentioned herein, or which has as its purpose an interest to cause the advertised product to be used or purchased because of this publication.

References

Anderson, D. M., D. W. Townsend, D. J. McGillicuddy, and J. T. Turner [eds.]. 2005. The ecology and oceanography of toxic *Alexandrium fundyense* blooms in the Gulf of Maine. Deep-Sea Res. II **52:** 2365–2876, doi:10.1016/j.dsr2.2005.08.001

Babin, M., C. S. Roesler, and J. J. Cullen [eds.]. 2008. Real-time coastal observing systems for ecosystem dynamics and harmful algal blooms. UNESCO Publishing.

———, and others. 2005. New approaches and technologies for observing harmful algal blooms. Oceanography **18:** 210–227.

Bakun, A. 1973. Coastal upwelling indices, west coast of North America, 1946–71. Spec. Sci. Rep. Fisheries, U.S. Department of Commerce, National Oceanic and Atmospheric Administration, National Marine Fisheries Service. 671.

Blasco, D., M. Levasseur, E. Bonneau, R. Gelinas, and T. T. Packard. 2003. Patterns of paralytic shellfish toxicity in the St. Lawrence region in relationship with the abundance and distribution of *Alexandrium tamarense*. Sci. Mar. **67:** 261–278, doi:10.3989/scimar.2003.67n3261

Breaker, L. C., and W. W. Broenkow. 1994. The circulation of Monterey Bay and related processes. Oceanogr. Mar. Biol. Annu. Rev. **32:** 1–64.

Campbell, L., R. J. Olson, H. M. Sosik, A. Abraham, D. W. Henrichs, C. J. Hyatt, and E. J. Buskey. 2010. First harmful *Dinophysis* (Dinophyceae, Dinophysiales) bloom in the U.S. is revealed by automated imaging flow cytometry. J. Phycol. **46:** 66–75, doi:10.1111/j.1529-8817.2009.00791.x

Casper, E. T., S. S. Patterson, P. Bhanushali, A. Farmer, M. Smith, D. P. Fries, and J. H. Paul. 2007. A handheld NASBA analyzer for the field detection and quantification of *Karenia brevis*. Harmful Algae **6:** 112–118, doi:10.1016/j.hal.2006.11.001

Cullen, J. J., and R. W. Eppley. 1981. Chlorophyll maximum layers of the Southern California Bight and possible mechanisms of their formation and maintenance. Oceanol. Acta **4:** 23–32.

Curtiss, C. C., G. W. Langlois, L. B. Busse, F. Mazzillo, and M. W. Silver. 2008. The emergence of *Cochlodinium* along the California Coast (USA). Harmful Algae **7:** 337–346, doi:10.1016/j.hal.2007.12.012

Doucette, G. J., and others. 2009. Remote, subsurface detection of the algal toxin domoic acid onboard the Environmental Sample Processor: Assay development and field trials. Harmful Algae **8:** 880–888, doi:10.1016/j.hal.2009.04.006

Franks, P. J. S. 1995. Thin layers of phytoplankton: A model of formation by near-inertial wave shear. Deep-Sea Res. I **42:** 75–91, doi:10.1016/0967-0637(94)00028-Q

Glibert, P., and G. Pitcher [eds.]. 2001. GEOHAB. Global ecology and oceanography of harmful algal blooms, science plan. Scientific Committee on Ocean Research.

Graham, W. M., and J. L. Largier. 1997. Upwelling shadows as nearshore retention sites: The example of northern Monterey Bay. Cont. Shelf Res. **17:** 509–532, doi:10.1016/S0278-4343(96)00045-3

Greenfield, D. I., R. Marin, III, S. Jensen, E. Massion, B. Roman, J. Feldman, and C. Scholin. 2006. Application of Environmental Sample Processor (ESP) methodology for quantifying *Pseudo-nitzschia australis* using ribosomal RNA-targeted probes in sandwich and fluorescent in situ hybridization formats. Limnol. Oceanogr.: Methods **4:** 426–435, doi:10.4319/lom.2006.4.426

———, and others. 2008. Field applications of the second-generation Environmental Sample Processor (ESP) for remote detection of harmful algae: 2006–2007. Limnol. Oceanogr.: Methods **6:** 667–679, doi:10.4319/lom.2008.6.667

Holm-Hansen, O., A. F. Amos, and C. D. Hewes. 2000. Reliability of estimating chlorophyll *a* concentrations in Antarctic waters by measurement of in situ chlorophyll *a* fluorescence. Mar. Ecol. Prog. Ser. **196:** 103–110, doi:10.3354/meps196103

Janowitz, G., and S. D. Kamykowski. 2006. Modeled *Karenia brevis* accumulation in the vicinity of a coastal nutrient front. Mar. Ecol. Prog. Ser. **314:** 49–59, doi:10.3354/meps314049

Jessup, D. A., and others. 2009. Mass stranding of marine birds caused by a surfactant-producing red tide. PLoS ONE **4:** e4550, doi:10.1371/journal.pone.0004550

Jester, R., K. Lefebvre, G. Langlois, V. Vigilant, K. Baugh, and M. W. Silver. 2009. A shift in the dominant toxin-producing algal species in central California alters phycotoxins in food webs. Harmful Algae **8:** 291–298, doi:10.1016/j.hal.2008.07.001

Jewett, E. B., C. B. Lopez, Q. Dortch, S. M. Etheridge, and L. C. Backer. 2008. Harmful algal bloom management and response: Assessment and plan. Interagency Working Group on Harmful Algal Blooms, Hypoxia, and Human Health of the Joint Subcommittee on Ocean Science and Technology. Available online at http://www.cop.noaa.gov/stressors/extremeevents/hab/habhrca/HABMngmt_resp_9_08.pdf

Johnson, K. S., and L. J. Coletti. 2002. In situ ultraviolet spectrophotometry for high resolution and long term monitoring of nitrate, bromide and bisulfide in the ocean. Deep-Sea Res. I **49:** 1291–1305, doi:10.1016/S0967-0637(02)00020-1

Joint, I., J. Lewis, J. Aiken, R. Proctor, G. Moore, W. Higman, and M. Donald. 1997. Interannual variability of PSP outbreaks on the northeast UK coast. J. Plankton Res. **19:** 937–956, doi:10.1093/plankt/19.7.937

Jones, W. J., C. Preston, R. Marin, III, C. Scholin, and R. Vrijenhoek. 2008. A robotic molecular method for in situ detection of marine invertebrate larvae. Mol. Ecol. Resour. **8:** 540–550, doi:10.1111/j.1471-8286.2007.02021.x

Kudela, R. M., J. P. Ryan, M. D. Blakely, J. Q. Lane, and T. D. Peterson. 2008. Linking the physiology and ecology of *Cochlodinium* to better understand harmful algal bloom events: A comparative approach. Harmful Algae **7:** 278–292, doi:10.1016/j.hal.2007.12.016

Lechuga-Deveze, C. H., and M. L. Morquecho-Escamilla. 1998. Early spring potentially harmful phytoplankton in Bahia Concepcion, Gulf of California. Bull. Mar. Sci. **63:** 503–512.

Li, Y., R. He, D. J. McGillicuddy, D. M. Anderson, and B. A. Keafer. 2009. Investigation of the 2006 *Alexandrium fundyense* bloom in the Gulf of Maine: In-situ observations and numerical modeling. Cont. Shelf Res. **29:** 2069–2082, doi:10.1016/j.csr.2009.07.012

Maldonado, M. T., M. P. Hughes, E. L. Rue, and M. L. Wells. 2002. The effect of Fe and Cu on growth and domoic acid production by *Pseudo-nitzschia multiseries* and *Pseudo-nitzschia australis*. Limnol. Oceanogr. **47:** 515–526, doi:10.4319/lo.2002.47.2.0515

McManus, M. A., R. M. Kudela, M. W. Silver, G. F. Steward, P. L. Donaghay, and J. M. Sullivan. 2008. Cryptic blooms: Are thin layers the missing connection? Estuaries and Coasts **31:** 396–401, doi:10.1007/s12237-007-9025-4

Mikulski, C. M., and others. 2008. Development and field application of rRNA-targeted probes for the detection of *Cochlodinium polykrikoides* Margalef in Korean coastal waters using whole cell and sandwich hybridization formats. Harmful Algae **7:** 347–359, doi:10.1016/j.hal.2007.12.015

O'Halloran, C., M. W. Silver, T. R. Holman, and C. A. Scholin. 2006. *Heterosigma akashiwo* in central California waters. Harmful Algae **5:** 124–132, doi:10.1016/j.hal.2005.06.009

ORION Executive Steering Committee. 2005. Ocean observatories initiative science plan. Washington, DC. p. 102. Available from http://www.geo-prose.com/pdfs/ooi_science_plan.pdf

Pan, Y., S. S. Bates, and A. D. Cembella. 1998. Environmental stress and domoic acid production by *Pseudo-nitzschia*: A physiological perspective. Nat. Toxins **6:** 127–135, doi:10.1002/(SICI)1522-7189(199805/08)6:3/4<127::AID-NT9>3.0.CO;2-2

Pennington, J. T., and F. P. Chavez. 2000. Seasonal fluctuations of temperature, salinity, nitrate, chlorophyll and primary production at station H3/M1 over 1989–1996 in Monterey Bay, California. Deep-Sea Res. II **47:** 947–973, doi:10.1016/S0967-0645(99)00132-0

Petruncio, E. T., L. K. Rosenfeld, and J. D. Paduan. 1998. Observations of the internal tide in Monterey Canyon. J. Phys. Oceanogr. **28:** 1873–1903, doi:10.1175/1520-0485(1998)028<1873:OOTITI>2.0.CO;2

Pingree, R. D., P. R. Pugh, P. M. Holligan, and G. R. Forster. 1975. Summer phytoplankton blooms and red tides along tidal fronts in the approaches to the English Channel. Nature **258:** 672–677, doi:10.1038/258672a0

Preston, C. M., and others. 2009. Near real-time, autonomous detection of marine bacterioplankton on a coastal mooring in Monterey Bay, California, using rRNA-targeted DNA probes. Environ. Microbiol. **11:** 1168–1180, doi:10.1111/j.1462-2920.2009.01848.x

Ramp, S. R., J. D. Paduan, I. Shulman, J. Kindle, F. L. Bahr, and F. P. Chavez. 2005. Observations of upwelling and relaxation events in the northern Monterey Bay during August 2000. J. Geophys. Res. **110:** C07013, doi:10.1029/2004JC002538

Ramsdell, J. S., D. M. Anderson, and P. M. Glibert [eds.]. 2005. HARRNESS. Harmful algal research and response: A national environmental science strategy 2005–2015. Ecological Society of America.

Rhodes, L., A. Selwood, P. McNabb, L. Briggs, J. Adamson, R. van Ginkel, and O. Laczka. 2006. Trace metal effects on the production of biotoxins by microalgae. Afr. J. Mar. Sci. **28:** 393–397, doi:10.2989/18142320609504185

Rosenfeld, L. K., F. B. Schwing, N. Garfield, and D. E. Tracy. 1994. Bifurcated flow from an upwelling center: A cold water source for Monterey Bay. Cont. Shelf Res. **14:** 931–964, doi:10.1016/0278-4343(94)90058-2

Rue, E., and K. Bruland. 2001. Domoic acid binds iron and copper: A possible role for the toxin produced by the marine diatom *Pseudo-nitzschia*. Mar. Chem. **76:** 127–134, doi:10.1016/S0304-4203(01)00053-6

Ryan, J. P., F. P. Chavez, and J. G. Bellingham. 2005*a*. Physical-biological coupling in Monterey Bay, California: Topographic influences on phytoplankton ecology. Mar. Ecol. Prog. Ser. **287:** 23–32, doi:10.3354/meps287023

———, A. M. Fischer, R. M. Kudela, J. F. R. Gower, S. A. King, R. Marin, III, and F. P. Chavez. 2009. Influences of upwelling and downwelling winds on red tide bloom dynamics in Monterey Bay, California. Cont. Shelf Res. **29:** 785–795, doi:10.1016/j.csr.2008.11.006

———, M. A. McManus, J. D. Paduan, and F. P. Chavez. 2008*a*. Phytoplankton thin layers within coastal upwelling system fronts. Mar. Ecol. Prog. Ser. **354:** 21–34, doi:10.3354/meps07222

———, ———, and J. M. Sullivan. 2010*a*. Interacting physical, chemical and biological forcing of phytoplankton thin-layer variability in Monterey Bay, California. Cont. Shelf Res. **30:** 7–16, doi:10.1016/j.csr.2009.10.017

———, J. A. Yoder, and P. C. Cornillon. 1999. Enhanced chlorophyll at the shelfbreak of the Mid-Atlantic Bight and Georges Bank during the spring transition. Limnol. Oceanogr. **44:** 1–11, doi:10.4319/lo.1999.44.1.0001

———, and others. 2005*b*. Coastal ocean physics and red tides, an example from Monterey Bay, California. Oceanography **18:** 246–255.

———, and others. 2008*b*. A coastal ocean extreme bloom incubator. Geophys. Res. Lett. **35:** L12602, doi:10.1029/2008GL034081

———, and others. 2010*b*. Recurrent frontal slicks of a coastal ocean upwelling shadow. J. Geophys. Res. **115:** C12070, doi:10.1029/2010JC006398

———, and others. 2010*c*. Mobile autonomous process sampling within coastal ocean observing systems. Limnol. Oceanogr.: Methods **8:** 394–402, doi:10.4319/lom.2010.8.394

Scholin, C., and others. 1999. Application of DNA probes and a receptor binding assay for detection of *Pseudo-nitzschia* (Bacillariophyceae) species and domoic acid activity in cultured and natural samples. J. Phycol. **35:** 1356–1367, doi:10.1046/j.1529-8817.1999.3561356.x

———, and others. 2009. Remote detection of marine microbes, small invertebrates, harmful algae and biotoxins using the Environmental Sample Processor (ESP). Oceanography **22:** 158–167.

Scholin, C. A., and others. 2000. Mortality of sea lions along the central California coast linked to a toxic diatom bloom. Nature **403:** 80–84, doi:10.1038/47481

Smayda, T. J. 2002. Turbulence, watermass stratification and harmful algal blooms: An alternative view and frontal zones as pelagic seed banks. Harmful Algae **1:** 95–112, doi:10.1016/S1568-9883(02)00010-0

Sullivan, J. M., P. L. Donaghay, and J. E. B. Rines. 2010. Coastal thin layer dynamics: Consequences to biology and optics. Cont. Shelf Res. **30:** 50–65, doi:10.1016/j.csr.2009.07.009

Tester, P. A., and K. A. Steidinger. 1997. *Gymnodinium breve* red tide blooms: Initiation, transport, and consequences of surface circulation. Limnol. Oceanogr. **42:** 1039–1051, doi:10.4319/lo.1997.42.5_part_2.1039

Trainer, V. L., B. M. Hickey, and E. J. Schumacker. 2003. Results from the Olympic Region Harmful Algal Bloom (ORHAB) project on the Washington State coast. The value of a collaborative project. J. Shellfish Res. **22:** 608–609.

———, and others. 2000. Domoic acid production near California coastal upwelling zones, June 1998. Limnol. Oceanogr. **45:** 1818–1833, doi:10.4319/lo.2000.45.8.1818

———, and others. 2009. Variability of *Pseudo-nitzschia* and domoic acid in the Juan de Fuca eddy region and its adjacent shelves. Limnol. Oceanogr. **54:** 289–308, doi:10.4319/lo.2009.54.1.0289

Woodson, C. B., and others. 2007. Local diurnal upwelling driven by sea breezes in northern Monterey Bay. Cont. Shelf Res. **27:** 2289–2302, doi:10.1016/j.csr.2007.05.014

———, and others. 2009. Northern Monterey Bay upwelling shadow front: Observations of a coastally and surface-trapped buoyant plume. J. Geophys. Res. **114:** C12013, doi:10.1029/2009JC005623

Zhang, Y., and J. G. Bellingham. 2008. An efficient method of selecting ocean observing locations for capturing the leading modes and reconstructing the full field. J. Geophys. Res. **113:** C04005, doi:10.1029/2007JC004327

———, R. S. McEwen, J. P. Ryan, and J. G. Bellingham. 2010. Design and tests of an adaptive triggering method for capturing peak samples in a thin phytoplankton layer by an autonomous underwater vehicle. IEEE J. Oceanic Eng. **35:** 785–796, doi:10.1109/JOE.2010.2081031

Associate editor: Heidi M. Sosik

Received: 13 September 2010
Accepted: 23 February 2011
Amended: 23 March 2011